Coupling matrix-based co-design of filter-oscillators

Gao, Yang; Shen, Fazhong; Qiao, Yingying; Guo, Haizhong; Li, Lei; Zhang, Fan; Wang, Yi

DOI:
10.1109/LMWC.2022.3146181

Coupling Matrix Based Co-Design of Filter-Oscillators

Yang Gao, *IEEE*, *Member*, Fazhong Shen, Yingying Qiao, Haizhong Guo, Lei Li, Fan Zhang, *IEEE*, *Member*, and Yi Wang, *IEEE*, *Senior Member*

***Abstract*—This letter presents a methodology of designing integrated filter-oscillators using the coupling matrix technique. The *N*+4 coupling matrix is developed for the first time to describe the filter-oscillator topology. Accordingly, the corresponding group delay, loop gain, loop phase and complex quality factor of the feedback filter can be calculated using the matrix. This helps rapidly predict oscillating frequencies at group delay or complex quality factor peak frequencies to achieve lower phase noise. Moreover, since the transistor and the transmission line entries are incorporated in the coupling matrix, the physical geometries can be directly determined, resulting in improved design efficiency. Two third-order filter-oscillators are implemented at 2.91 GHz (group delay peak) and 3.15 GHz (complex quality factor peak) frequencies, respectively. The developed filter-oscillators are measured with -121 dBc/Hz and -145 dBc/Hz phase noise at 1 MHz offset frequency, validating this coupling matrix based co-design approach.**

***Index Terms*—Active coupling matrix, transistor, resonator, filter-oscillator.**

I. Introduction

MICROWAVE oscillator is mainly employed as a local-oscillating (LO) signal source in radar and wireless communication systems [1]-[3]. It can be designed with an integrated bandpass filter in the feedback loop as the frequency-selective element. The integrated filter, formed of multiple resonators, can significantly improve the oscillator's phase noise performance by adding more resonators [1]-[2]. In order to maximize phase-noise performance, the oscillating frequency is often determined at the peaks of the group delay or the complex quality factor, according to the phase-noise figure-of-merit (PNFOM) formula [2].

Conventionally, in a filter-oscillator, the filter and the oscillator are designed separately as follows: 1) the filter is designed, and then the oscillation frequency can be determined by the simulated filter response and the PNFOM formula; 2) the transistor amplifier is designed to provide the required gain, and its phase response is obtained; 3) the transmission line (TL) in the feedback loop is determined by cascading the filter and the amplifier to fulfil the "Barkhausen" oscillation criteria [2]. The design procedure is shown in Fig. 1. All the above steps should apply time-consuming electromagnetic (EM) simulation to obtain the desired results.

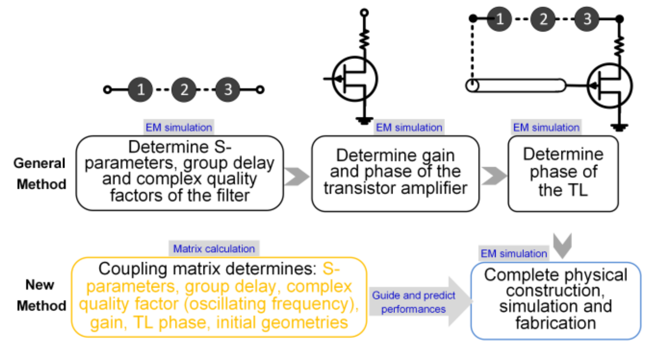

Fig. 1 Filter-oscillators design using conventional and the coupling matrix based method.

In this work, the classic filter synthesis based on the coupling matrix is extended and applied in the design of integrated filter-oscillators. The new *N*+4 coupling matrix incorporates transistor elements (corresponding to gain) and TL entries (corresponding to electrical length). It can calculate the loop gain, phase, *S*-parameters, complex quality factor and group delay. Oscillation frequencies corresponding to the group delay peak or the complex quality factor peak can also be predicted. It can be rapidly calculated using the coupling matrix, instead of modelling and simulating complex physical structures. Moreover, the physical construction and dimensioning of the integrated circuit can be guided by a single coupling matrix as an entity. The independent design steps using EM simulations are eliminated. This is not possible with conventional design techniques. The coupling-matrix based co-design approach streamlines the design procedure and can be used to improve the design efficiency.

II. Coupling Matrix for Filter-Oscillator Design

The topology and the circuit of the filter-oscillator are schematically illustrated in Fig. 2(a) and (b). The feedback transfer function $H(j\omega)$, as in a general oscillator model (Fig. 2(c)) is realized by a resonator-based filter. The coupling topology is shown in Fig. 2(a), where the black circles denote the resonators. The grey circles indicate the TLs, treated as non-resonant nodes, providing loop phase control. The triangle represents the transistor amplifier and Y_L is the 50 Ω output load. For the equivalent circuit in Fig. 2(b), the filter is formed of parallel *LC* resonators coupled by *J* inverters. Admittance Y_T

Manuscript received Sept. 14, 2021; revised Nov. 28, 2021; accepted Jan. 21, 2022.This work was supported by the National Key Scientific Instruments and Equipment Development program (NO. 6202780147). (*Corresponding author: Lei Li and Fan Zhang*)

Y. Gao, F. Shen, Y. Qiao, H. Guo and L. Li are with Henan Key Laboratory of Diamond Optoelectronic Material and Devices, School of Physics and Microelectronics, Zhengzhou University, Zhengzhou, China, 450001.

F. Zhang is with Ganide Technology Co., Ltd., Chengdu, China, 610220.

Y. Wang is with Department of Electronic, Electrical and Systems Engineering, University of Birmingham, Birmingham, B15 2TT, UK.

Color versions of one or more of the figures in this letter are available online at http://ieeexplore.ieee.org.

Digital Object Identifier xxxxxxxxxxxxxxxxxx

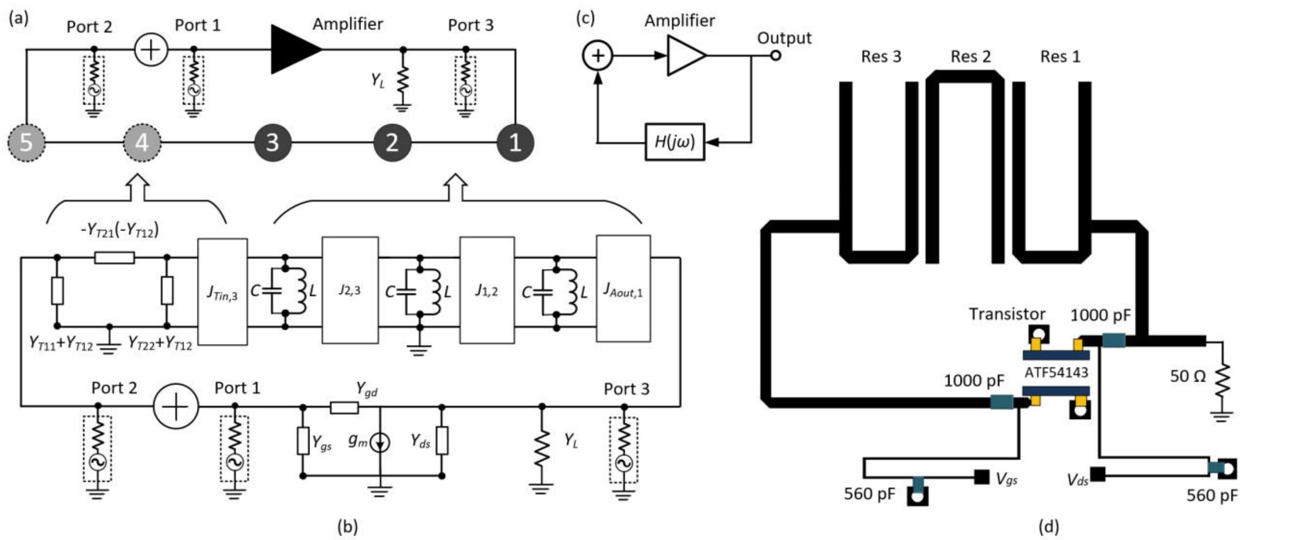

Fig. 2. (a) Filter-oscillator. (b) Equivalent lumped circuit of the filter-oscillator. Y_{gs}, Y_{gd}, and Y_{ds} are the admittances between transistor's gate, source and drain; g_m is the transconductance. Y_{T11}, Y_{T12}, Y_{T21}, and Y_{T22} are the admittance matrix elements of the TL sections. Port 1, port 2 and port 3 are the open-loop test ports. (c) Block diagram of a feedback oscillator. (d) Schematic of the filter-oscillator.

represents the TLs and the transistor is represented by the small-signal equivalent lumped circuit. In this example, we use a third-order filter (N = 3). In order to calculate the circuit responses, we add two probe ports (Port 1 and Port 2) at the ends.

Apply Kirchhoff's law at each node of the circuit and write down equations in matrix form. This impedance/admittance matrix of the network can be manipulated and transferred to the general coupling matrix [A], given in (1). The detailed matrix manipulation process is given in [4] and [5], and have been applied in our previous work of filter-amplifiers [5]-[7]. Different from the previous active matrices in [5]-[7], the newly synthesized coupling matrix includes the non-resonating nodes to represent TL. This is specifically useful in designing oscillators. Moreover, complex quality factors can be calculated to determine the oscillating frequencies. Note that the matrix [A] contains a passive submatrix [A_1] denoting the loop filter and an active submatrix [A_2] indicating the transistor.

$m_{i,j}$ (i, j=1 to N)is the inter-resonator normalized coupling coefficient in a conventional filter, which can be calculated from the g-values of the low-pass prototype [8]. The external coupling coefficients of the 1st resonator ($m_{1,TAin}$) and the 3rd resonator ($m_{3,Tin}$) can be calculated by

$$m_{1,TAin} = m_{Ain,1} = 1/\sqrt{q_{e1}}, \quad m_{3,Tin} = m_{Tin,3} = 1/\sqrt{q_{e3}} \qquad (2)$$

where q_{e1} and q_{e3} are normalized quality factors of the 1st and 3rd resonator and they also can be obtained according to the classic filter synthesis [8].

The non-resonance nodes (the TLs) are represented by the admittance Y_{T11}, Y_{T12}, Y_{T21} and Y_{T22} as

$$Y_{T11} = Y_{T22} = \frac{\cos\varphi}{j\sin\varphi} \qquad Y_{T12} = Y_{T21} = \frac{-1}{j\sin\varphi} \qquad (3)$$

where φ is the phase of the TL. The frequency variable p is defined by

$$p = j(\omega/\omega_0 - \omega_0/\omega) \qquad (4)$$

where ω is the angular frequency. The transistor's equivalent circuits can be extracted from the manufacturer datasheet.

As illustrated in Fig. 2(a), passive filter responses of reflection coefficient (S_{22}) and transmission coefficient (S_{32}), as well as the open-loop gain (S_{21}) can be calculated by

$$S_{22} = 2[A_1^{-1}]_{1,1} - 1, \quad S_{32} = 2[A_1^{-1}]_{n,1}, \; S_{21} = 2[A^{-1}]_{n,1} \qquad (5)$$

Here, n is the dimension of the matrix. The group delay can be expressed by [9]

$$\tau_g = \mathrm{Im}\left[\sum_{k=2}^{n+1} [A^{-1}]_{n,k}[A^{-1}]_{k,1} \Big/ [A^{-1}]_{n,1}\right] \qquad (6)$$

Referring to the complex quality factor (Q_{sc}) definition from the Lesson oscillator spectrum noise model [1], Q_{sc} can also be expressed by the coupling matrix. Since Q_{sc} was derived using the passive network [10], it is related to the submatrix [A_1] as

$$Q_{sc} = \frac{\omega_0}{2}\left|\frac{d}{d\omega}\ln\left(\frac{[A_1^{-1}]_{1,n}}{2[A_1^{-1}]_{1,1}\cdot[A_1^{-1}]_{1,n} - 2[A_1^{-1}]_{1,n}\cdot[A_1^{-1}]_{n,1}}\right)\right| \qquad (7)$$

Submatrix [A_2] Submatrix [A_1]

$$[A] = \begin{bmatrix} Y_{P1}+Y_{gs}+Y_{gd} & -Y_{gd} & 0 & 0 & 0 & 0 & 0 \\ g_m - Y_{gd} & Y_{gd}+Y_{ds}+Y_L & -jm_{Ain,1} & 0 & 0 & 0 & 0 \\ 0 & -jm_{1,Ain} & p & -jm_{1,2} & 0 & 0 & 0 \\ 0 & 0 & -jm_{2,1} & p & -jm_{2,3} & 0 & 0 \\ 0 & 0 & 0 & -jm_{3,2} & p & -jm_{3,Tin} & 0 \\ 0 & 0 & 0 & 0 & -jm_{Tin,3} & Y_{T11} & Y_{T12} \\ 0 & 0 & 0 & 0 & 0 & Y_{T21} & Y_{T22}+Y_{P2} \end{bmatrix} \qquad (1)$$

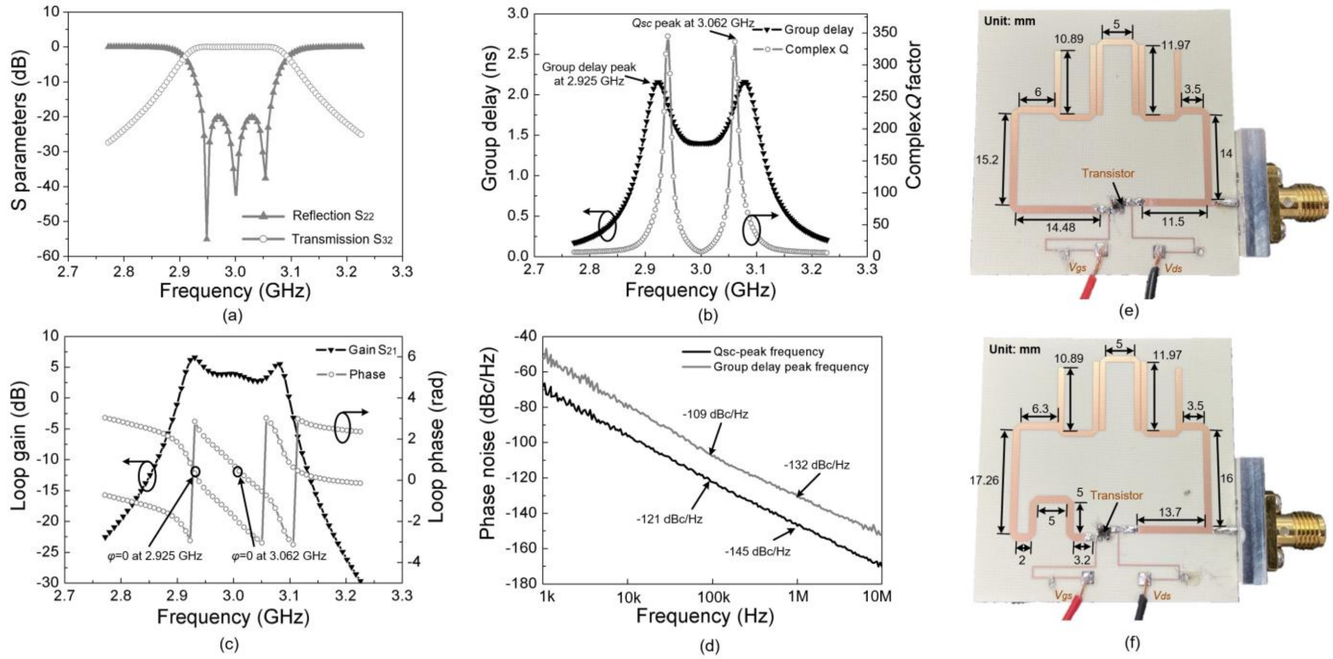

Fig. 3. Responses calculated using the coupling matrix: (a) S-parameters of the filter; (b) Complex Q-factor and group delay; (c) Loop gain and phase. (d) Measured phase noises of two oscillators designed at the Q_{sc}-peak and group-delay-peak. Photos of the oscillator at (e) 2.91 GHz (Q_{sc}-peak) and (f) 3.15 GHz (group-delay-peak).

TABLE I
SUMMARY OF THE RECENTLY REPORTED FILTER-OSCILLATORS

Ref.	BW (GHz)	f_0 (GHz)	P_{DC} (mW)	Eff. (%)	Phase Noise (dBc/Hz@1MHz)
[1]	n/a	8.05	22	10	-143.5
[2]	1.3-2.28	2.05	20	14.8	-148.3
[3]	1.45-2.45	2.05	6.1	35.9	−150.4
[12]	37.6-38.1	37.8	129.9	8.56	-112.3
[13]	2.45-2.46	2.46	24	14.1	-147
[14]	n/a	10.178	13.6	5.4	-135.4
[15]	n/a	2.004	45	18.4	-144.97
This	n/a	3.15	21	13.2	-145
work	n/a	2.91	21	13.5	-132

Our example is a 3-pole Chebyshev filter, with a center frequency f_0 of 3 GHz, 150 MHz bandwidth (FBW=0.05) and a return loss of 20 dB. The micostrip hairpin resonators are used to construct the bandpass filter, as illustrated in Fig. 2(d). The corresponding external Q is 17.03. The inter-resonator couplings are: $M_{1,2} = M_{2,1} = 0.0516$; $M_{2,3} = M_{3,2} = 0.0516$. The extraction procedure of the external Q and the coupling coefficients are introduced in [8]. The ATF-54143 transistor is used [11] and admittance parameters are: $Y_{gs} = 3.6843 + 2.2731j$, $Y_{gd} = 0.3030 + 0.4595j$, $Y_{ds} = 0.8920 + 2.0972j$ and $g_m = -15.2452 - 23.0591j$. The S-parameter response of the filter is given in Fig. 3(a). Substituting (1) into (6) and (7), the group delay and complex Q response can be calculated, as shown in Fig. 3(b). Note that the peaks of the complex Q are different from those of the group delay. According to [2], lower phase noise can be obtained for oscillation at the complex Q factor peaks than at the group delay peaks. Two oscillators are built at the complex Q peak and the group delay peak, respectively, and compared. They oscillate at 2.925 GHz and 3.062 GHz, respectively. Substitution of (1) into (5) yields the gain and phase response of the open-loop, as illustrated in Fig. 3(c). Note that the length of the TL is chosen to fulfil the loop phase of 0° or multiple of 360°. The loop gain of the oscillator should be greater than unity [2]. The loop phase and the corresponding TL electrical length can be obtained to be 1.77π and 1.08π, respectively.

III. FABRICATION AND MEASUREMENTS

Two filter-oscillators are fabricated on RO4003 substrate with a thickness of 0.508 mm and a dielectric constant of 3.38. Fig. 3(e) and (f) show the photographs of the manufactured oscillators. The output power measured at 3.15 GHz and 2.91 GHz are 4.4 dBm and 4.5 dBm after calibrating the cable and bias tee. The consumed DC power is 21 mW for both oscillators, corresponding to an efficiency of 13.2% and 13.5%, respectively. As shown in Fig. 3(d), the measured phase noises are -109 dBc/Hz and -132 dBc/Hz at 100 kHz and 1 MHz offset at group delay peak; -121 dBc/Hz and -145 dBc/Hz at Q_{sc} peak. The performances compared with other reported filter-oscillators are summarized in Table I. The oscillator operating at the Q_{sc} peak frequency achieves a 12 dB lower phase-noise, and this validates the integrated filter-oscillators design methodology using the coupling matrix technique.

IV. CONCLUSION

This letter presents a novel co-design method for filter-oscillators using a unified N+4 coupling matrix. All the key performance parameters, such as the complex quality factor, group delay, loop gain, and phase responses, can be calculated and predicted using the coupling matrix. As in the synthesis of conventional filters, it also facilities the construction and dimensioning of the filter-oscillator circuits, which can be used to improve design efficiencies for similar integrated circuits using a streamlined procedure. This coupling matrix based co-design technique is expected to be applied in many multi-functional microwave devices and systems.

REFERENCES

[1] J. Choi, M. Nick and A. Mortazawi, "Low phase-noise planar oscillators employing elliptic-response bandpass filters," *IEEE Trans. Microw. Theory Techn.*, vol. 57, no. 8, pp. 1959-1965, Aug. 2009

[2] C. Tseng and C. Chang, "Design of low phase-noise microwave oscillator and wideband VCO based on microstrip combline pandpass filters," *IEEE Trans. Microw. Theory Techn.*, vol. 60, no. 10, pp. 3151-3160, Oct. 2012

[3] A. Alburaikan, M. Aqeeli, X. Huang and Z. Hu, "Low phase noise free-running oscillator based on high selectivity bandpass filter using composite right/left-handed transmission line," *IEEE Microw. Wirel. Compon. Lett.*, vol. 26, no. 4, pp. 273-275, April 2016.

[4] R. J. Cameron, R. Mansour, and C. M Kudsia, *Microwave Filters for Communication Systems: Fundamentals, Design and Applications*. 1st. New York, NY, USA: Wiley, 2007. pp. 283-288.

[5] Y. Gao, J. Powell, X. Shang and M. J. Lancaster, "Coupling matrix-based design of waveguide filter amplifiers," *IEEE Trans. Microw. Theory Techn.* vol. 66, no. 12, pp. 5300-5309, Dec. 2018.

[6] Y. Gao, F. Zhang, X. Shang, C. Guo, J. Powell, Y. Wang, and M. J. Lancaster, "Integrated waveguide filter amplifier using the coupling matrix technique," *IEEE Microw. Wirel. Compon. Lett.*, vol. 29, no. 4, pp. 267-269, 2019.

[7] Y. Gao X. Shang, X. Lv *et al.*, "Substrate integrated waveguide filter-amplifier design using active coupling matrix technique," *IEEE Trans. Microw. Theory Techn.*, vol. 68, no. 5, pp. 1706-1716, 2020.

[8] J. S. Hong and M. J. Lancaster, *Microstrip Filters for RF/Microwave Applications*. New York, NY, USA: Wiley, 2001.

[9] S. Amari, "Synthesis of cross-coupled resonator filters using an analytical gradient-based optimization technique," *IEEE Trans. Microw. Theory Techn.*, vol. 48, no. 9, pp. 1559-1564, Sept. 2000.

[10] T. Ohira, "Rigorous Q-factor formulation for one- and two-port passive linear networks from an oscillator noise spectrum viewpoint," *IEEE Trans. Circuits Syst. II, Exp. Briefs*, vol. 52, no. 12, pp. 846–850, Dec. 2005.

[11] Broadcom Limited, U.S. [Online]. Available: www.broadcom.com.

[12] C. Chang, C. Tseng and H. Chang, "A new monolithic Ka-band filter-based voltage-controlled oscillator using 0.15 um GaAs pHEMT technology," *IEEE Microw. Wirel. Compon. Lett.*, vol. 24, no. 2, pp. 111-113, Feb. 2014.

[13] C. H. Tseng and T. S. Huang, "Microwave voltage-controlled oscillator with harmonic-suppressed stepped-impedance-resonator filter," *IEEE Trans. Syst. II: Expr. Briefs*, vol. 64, no. 5, pp. 520-524, May 2017.

[14] T. Duong, W. Hong, V. Tran *et al.*, "An alternative technique to minimize the phase noise of X-band oscillators using improved group delay SIW filters," *IEEE Microw. Wirel. Compon. Lett.*, vol. 27, no. 2, pp. 153-155, Feb. 2017.

[15] Z. Cai, X. Tang, Z. Li *et al.*,, "A low phase noise differential oscillator employing stub-loaded nested split-ring resonator inspired balanced bandpass filter," *2019 IEEE MTT-S Intern.Microw. Symp. (IMS),* 2019, pp. 967-970.